

Synthesis of New Pharmacophore Scaffolds

A Major Qualifying Project submitted for review to the faculty of
WORCESTER POLYTECHNIC INSTITUTE

In partial fulfillment of the requirements for the
Degree of Bachelor of Science

Submitted by:

Emily Domingue

Matthew Fusco

Project Advisor:

Dr. James P. Dittami, WPI Professor

Abstract

The photo-initiated cyclization of aryl-vinyl ethers has been shown to create multicyclic natural product-like scaffolds with predicted biological activity. Utilizing this method, one can construct up to three fused rings and six chiral centers in a single experimental operation. A cheminformatics analysis of these structures has identified scaffolds which are likely to interact with proteins. Using these predictions, our group has constructed two scaffolds with predicted biological activity.

Acknowledgements

We would like to thank Dr. James P. Dittami for his continued guidance and support, and the use of his laboratory and resources. We would also like to thank Alicia Morgan for her amazing support and help throughout the entire year.

Table of Contents

Abstract	i
Acknowledgements.....	ii
List of Figures.....	iv
1. Introduction	1
2. Background.....	2
<i>Schultz</i> Photo-Initiated Cycloaddition.....	2
Intramolecular Addition Reactions of Carbonyl Ylides	3
Similarity Ensemble Approach.....	4
Predicted Protein Targets	6
3. Results and Discussion	8
4. Experimental	13
3-ethoxy-2-cyclohexen-1-one.....	13
3-[2-(1,3-Dioxan-2-yl)ethyl]-2-cyclohexen-1-one.....	15
6-(2-(1,3-dioxan-2-yl)-7-oxabicyclo[4.1.0]heptan-2-one.....	16
3-(2-(1,3-dioxan-2-yl)ethyl)-2-(3-methoxyphenoxy)cyclohexenone	17
3-(2-(1,3-dioxan-2-yl)ethyl)-2-(3,5-dimethoxyphenoxy)-cyclohex-2-enone	18
3-(2-(3-methoxyphenoxy)-3-oxocyclohex-1-en-1-yl)propanal.....	19
3-(2-(3,5-dimethoxyphenoxy)-3-oxocyclohex-1-en-1-yl)propanal.....	20
OmMAA2	21
OdMAA.....	22
References	23
Appendices.....	25
Appendix A: NMR Data	25

List of Figures

Figure 1: Photo-initiated ylide-olefin cycloaddition.....	2
Figure 2: Photocyclization and subsequent intramolecular ylide-alkene addition to the side-chain alkene	3
Figure 3: Natural product-like scaffolds synthesized by the Dittami group	4
Figure 4: Structures predicted to interact with PPAR	6
Figure 5: Formation of epoxide precursor from 1,3-cyclohexanedione via a three step synthesis	8
Figure 6: Formation of aryl-vinyl ether precursor for photocyclization.....	9
Figure 7: Structure of aryl-vinyl ether with key proton signals (Labeled a-e)	10
Figure 8: Formation of the photocyclic scaffold via an intramolecular addition of 6a	10
Figure 9: Formation of deprotected aryl-vinyl ether precursor for photocyclization.....	11
Figure 10: Formation of the photocyclic scaffold via an intramolecular addition of 6b.....	12

1. Introduction

Upon the 1903 discovery that drugs bind to certain cell receptors, Paul Elhrich coined the term “pharmacophore” to describe drug molecular groups that are responsible for eliciting a biological response. Scientists have since been searching for “magic bullet” pharmacophores which target disease causing microbes without affecting the body.¹ Early phases of drug discovery involved testing the biological activity of natural product analogs.² For instance Morphine is a narcotic analgesic that was isolated from the opium poppy. Modifications of opium through bioisosteric replacements have led to other opiates. The rationale for using bioisosteric replacements in drug design comes from the known physiochemical similarities between molecular groups.³ Although Morphine was discovered in the 1800s, Morphine derivatives are still under investigation as new drugs.⁴

There are several challenges facing drug design including unwanted side effects or structural elements that lead to either rapid degradation or excretion from the body.⁵ The role of natural products in contemporary drug design has waned due to the advent of high-throughput screening.⁶ Natural product derived chemical scaffolds can be modified and inputted into compound libraries. Computational analysis can then be used to screen the compound libraries against protein targets to predict interactions and several algorithms have been developed for this purpose. This method is useful in predicting side-effects of potential pharmacophores prior to synthesis of the compounds.⁷

¹ Guner, O. F. (Ed.). (2000). *Pharmacophore perception, development, and use in drug design* International University Line.

² Harvey, A. L. (2008). Natural products in drug discovery. *Drug Discovery Today*, 13(19), 894-901.

³ Patani, G. A., & LaVoie, E. J. (1996). Bioisosterism: A rational approach in drug design. *Chemical Reviews*, 96(8), 3147-3176.

⁴ Casey, A. F., & Parfitt, R. T. (1986). *Opioid analgesics: Chemistry and receptors*. New York: Plenum Publishing Corporation.

⁵ Patani, G. A., & LaVoie, E. J. (1996). *Bioisosterism: A rational approach in drug design*. Easton: American Chemical Society.

⁶ Koehn, F. E., & Carter, G. T. (2005). The evolving role of natural products in drug discovery. *Nature Reviews Drug Discovery*, 4(3).

⁷ Grabowski, K., Baringhaus, K., & Schneider, G. (2008). Scaffold diversity of natural products: Inspiration for combinatorial library design. *Natural Product Reports*, 25(5), 892.

2. Background

The pharmacophore scaffolds synthesized in this study are based on the photo-initiated cycloaddition reaction pioneered by Schultz and further development by the Dittami group. Chemo-informatics analysis of these multicyclic compounds has provided predicted scaffold-protein interactions.

Schultz Photo-Initiated Cycloaddition

Arthur G. Schultz pioneered a photo-initiated ylide-olefin cycloaddition as shown in below in Figure 1.

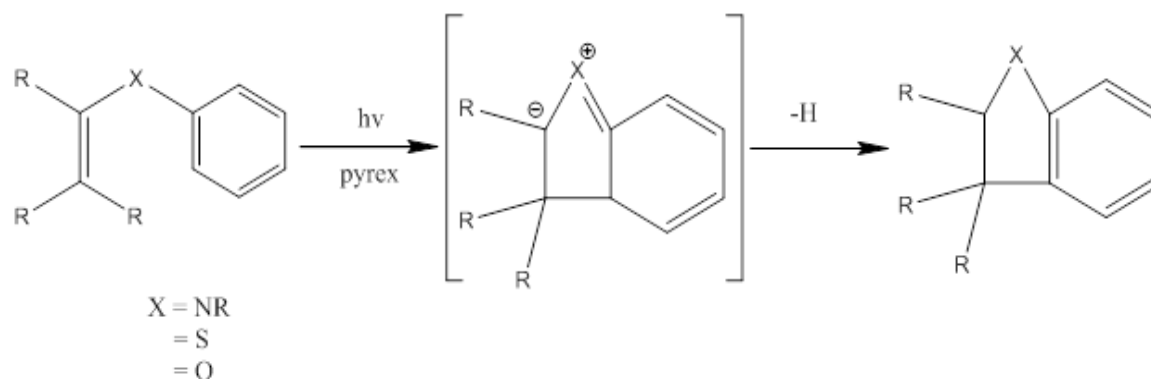


Figure 1: Photo-initiated ylide-olefin cycloaddition⁸

Schultz observed that the above reaction proceeds by a six-electron electrocyclic rearrangement involving an aryl and vinyl group linked by a heteroatom (X). The heteroatom is an atom that has an unshared electron pair such as an amine group (NR), sulfur group (S), or oxygen group (O). When exposed to Pyrex-filtered ultraviolet (UV) light under degassed conditions the ylide-alkene intermediate forms and is followed by a series of hydrogen shifts that result in the formation of a carbon-carbon bond to an aromatic ring.

⁸ Schultz, A. G. (1983). Photochemical six-electron heterocyclization reactions. *Accounts of Chemical Research*, 16(6), 210-218.

Intramolecular Addition Reactions of Carbonyl Ylides

The Dittami group explored aryl vinyl ethers, aryl vinyl thiols, and aryl vinyl amines bearing a pendant alkene group and found that these can undergo both photocyclization and subsequent intramolecular ylide-alkene additions to the side-chain alkene under specific conditions.⁹

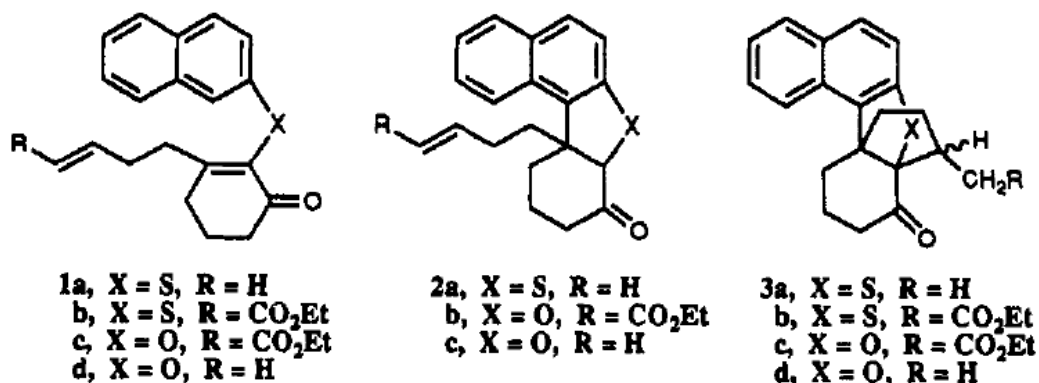


Figure 2: Photocyclization and subsequent intramolecular ylide-alkene addition to the side-chain alkene¹⁰

The photolysis with Pyrex-filtered light was performed at temperatures ranging from -78°C to 110°C. The results of these experiments varied depending on reaction conditions, the aryl group, and the side chain of the starting compound. For example, compound 1a (shown in Figure 2) favors the formation of the hydrogen shift product 2a when exposed to Pyrex-filtered UV light at low temperatures (-78°C to 0°C), but favors the intramolecular addition product 3a when exposed to UV light at high temperatures (110°C). When the vinyl group (R) is substituted with an ethyl ester as in 1b, photolysis forms the intramolecular addition product 3b at both high and low temperature conditions.¹¹

The findings of this study are significant because it provides a method for creating up to three new rings and six new chiral centers in one reaction. It also demonstrates that a wide range of compounds can be produced by varying reaction conditions and starting materials. Furthermore, this

⁹ Dittami, J. P., Ware, R., Nie, X. Y., Nie, H., Ramanathan, H., Breining, S., Reiche, P. (1991). Intramolecular addition reactions of carbonyl ylides formed during photocyclization of aryl vinyl ethers. *The Journal of Organic Chemistry*, 56(19), 5572-5578.

¹⁰ Ibid.

¹¹ Ibid.

method of synthesizing complex multicyclic systems may prove important in creating multicyclic natural product-like scaffolds. Such scaffolds include Morphine, Huperzine A, Huperzine B, and Mesimbrine. Figure 3 shows the similarities between natural products and scaffolds synthesized by the Dittami group. Synthesis of natural product-like scaffolds could lead to the creation of new pharmacophores.

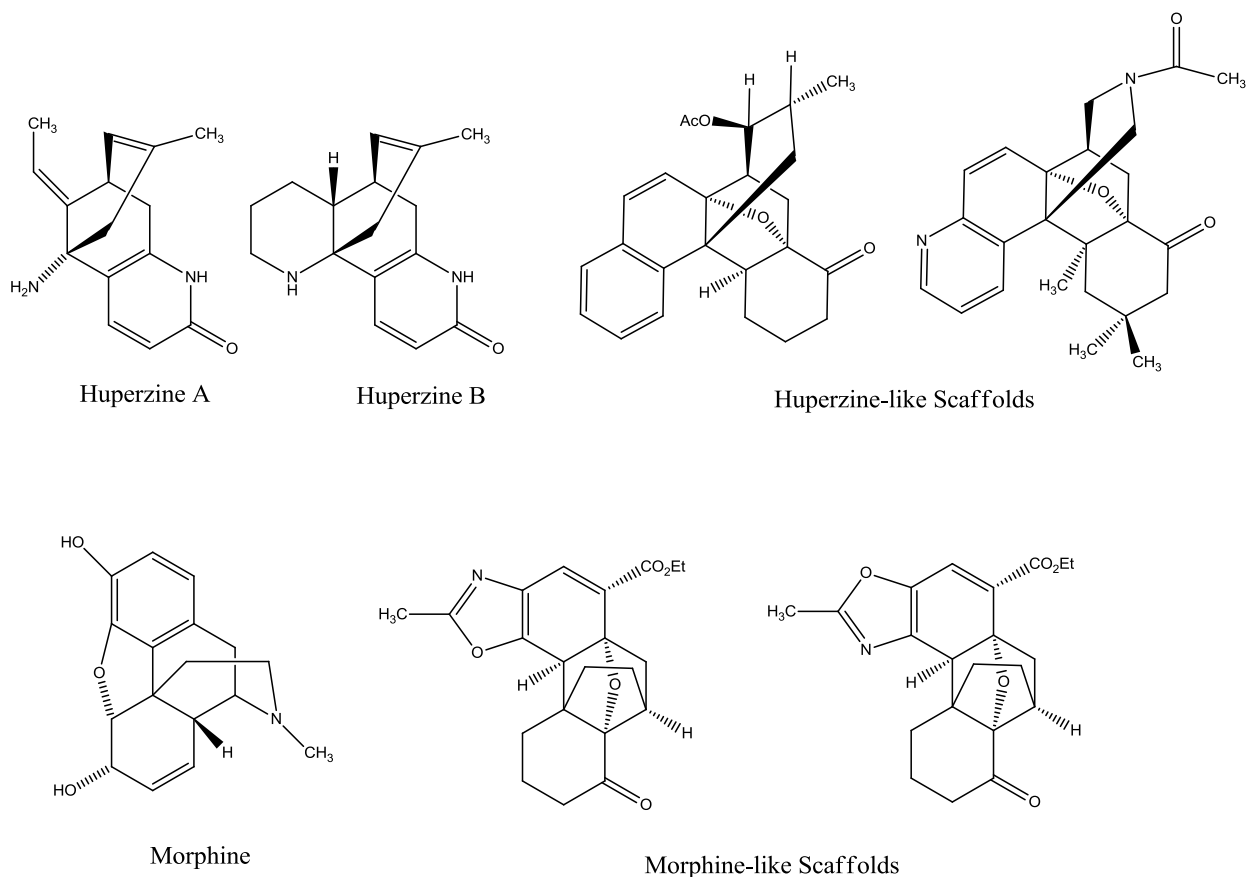


Figure 3: Natural product-like scaffolds synthesized by the Dittami group¹²

¹² Dittami, J. P. (2003). Explorations of the heteroatom directed photoarylation reaction. A review of the photoinitiated intramolecular cycloaddition reactions of ylide systems. *Cheminform*, 34(45)

Similarity Ensemble Approach

Utilizing high throughput screening to predict drug-target interactions is critical in drug development to increase both time and cost efficiency.¹³ The Shoichet group at the University of California San Francisco has pioneered a novel approach to predicting new targets for known drugs. This Similarity Ensemble Approach (SEA) compares drugs to protein targets by assessing the similarity between the drug and the ligand set that binds to a specific protein. In a recent publication, this research group compared 3,665 known drugs to 65,241 ligands of 246 protein targets from the MDL Drug Data Report (MDDR) database. The drug-ligand pair comparisons were quantified by expectation values (e-values) in which a lower e-value corresponds to a greater similarity between drug and ligand. Out of the 901,590 drug-ligand comparisons, 6,928 pairs yielding e-values of less than 1×10^{-10} . Thirty of these predictions were chosen to be subjected to a binding assay on the basis that the associations were not previously known and the pair was experimentally available. Twenty-three of the thirty drug-target pairs tested (77%) resulted in new associations.¹⁴

Scaffolds from the Dittami lab were analyzed by the SEA method. Two algorithms, Daylight and Extended Connectivity Fingerprint (ECFP), were used in this process. The Daylight algorithm created by Daylight Chemical Information Systems inputs the chemical molecules in a line notation that represents each bonded atom. The linear patterns are created at varying lengths. For example the notation 0 signifies zero bonds and 7 signifies a seven-atom bond length. Structural patterns of the molecules such as bond type, cyclic compounds, ionic bonds, etc. are notated. The Daylight algorithm compares molecules based on their linear atom sequences and the structural patterns.¹⁵ ECFP represents molecules by circular pathways rather than linear connectivity. ECFP is effective in representing the topological features of a compound. Using circular pathways is generally more selective than linear analysis.¹⁶

¹³ Cao, D., Liu, S., Xu, Q., Lu, H., Huang, J., Hu, Q., & Liang, Y. (2012). Large-scale prediction of drug-target interactions using protein sequences and drug topological structures. *Analytica Chimica Acta*, 752, 1.

¹⁴ Keiser, M. J., Tran, T. B., Whaley, R., Glennon, R. A., Hert, J., Thomas, K. L. H., Matos, R. C. (2009). Predicting new molecular targets for known drugs. *Nature*, 462(7270), 175-181.

¹⁵ Daylight theory manual.

¹⁶ Rogers, D., & Hahn, M. (2010). Extended-connectivity fingerprints. *Journal of Chemical Information and Modeling*, 50(5), 742

Predicted Protein Targets

The Dittami group submitted 41 drug scaffolds for SEA analysis. The Daylight algorithm predicts 169 target-scaffold interactions involving 50 protein targets and 20 drug scaffolds with e-values of 1×10^{-7} or lower. The ECFP algorithm predicts 9 target-scaffold interactions involving 3 targets and 9 scaffolds with the same e-value cut-off. Using the Daylight algorithm, the scaffold-target interaction with the lowest e-value (2.41×10^{-44}) involves the peroxisome proliferator-activated receptor alpha (PPAR). PPAR resulted in a total of ten scaffold hits using SEA analysis, nine of which have low e-values ranging from 1.01×10^{-36} to 1.25×10^{-40} . The focus of this study is to synthesize these scaffolds and valid these predictions by biological testing. The scaffolds are depicted in Figure 4 below and labeled with a code name designated by the Dittami lab.

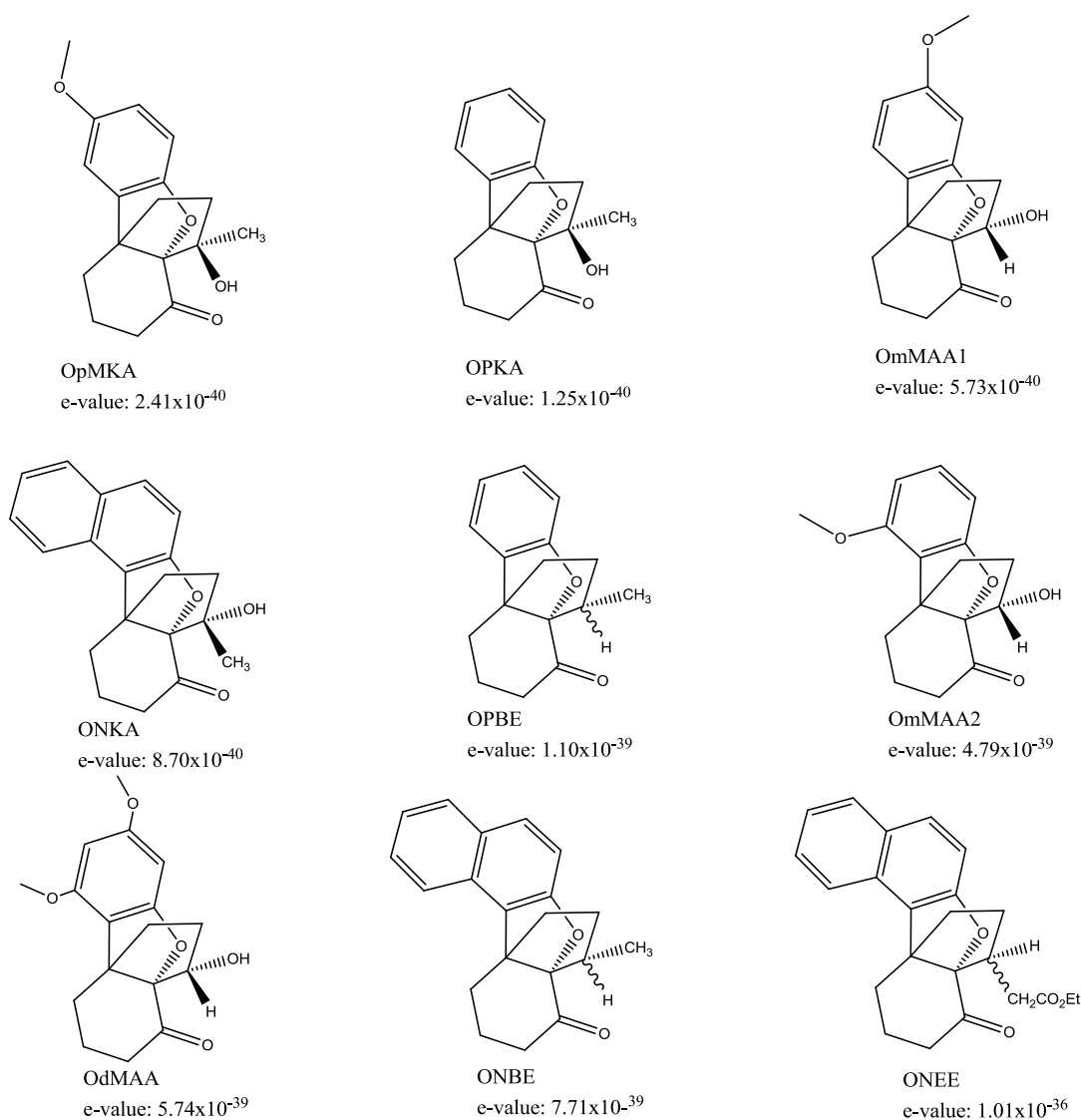


Figure 4: Structures predicted to interact with PPAR

PPAR is a nuclear hormone receptor that regulates transcription of target genes based on ligand binding.¹⁷ Some of the cellular functions regulated by PPAR include glucose, lipid, and cholesterol metabolism. It also plays a key role in regulating inflammatory responses of the cardiovascular system and the liver. PPAR may be an ideal target in treating metabolic syndromes such as diabetes and obesity or cardiovascular diseases.¹⁸

Using the ECFP algorithm, the scaffold-target interaction with the lowest e-value (3.81×10^{-19}) involves NAD-dependent histone deacetylase SIR2. SIR2 is a yeast deacetylase and the closest human homolog is the deacetylase SIRT1. SIRT1 has been shown to form a complex with PPAR alpha preventing cardiac hypertrophy, metabolic dysregulation, and inflammation.¹⁹ This may be a good indicator that the scaffolds predicted to interact with both PPAR alpha and SIR 2 including ONBE, ONKA, and ONEE (see Figure 4), may interact in this cardiac pathway.

¹⁷ Mandard, S., Müller, M., & Kersten, S. (2004). Peroxisome proliferator-activated receptor alpha target genes. *Cellular and Molecular Life Sciences : CMLS*, 61(4), 393.

¹⁸ Fruchart, J. (2007). Novel peroxisome proliferator activated receptor-alpha agonists. *The American Journal of Cardiology*, 100(11 A), n41.

¹⁹ Planavila, A., Iglesias, R., Giralt, M., & Villarroya, F. (2011). Sirt1 acts in association with PPAR α to protect the heart from hypertrophy, metabolic dysregulation, and inflammation. *Cardiovascular research*, 90(2), 276-284

3. Results and Discussion

The requisite scaffolds were synthesized according to the published procedure.²⁰

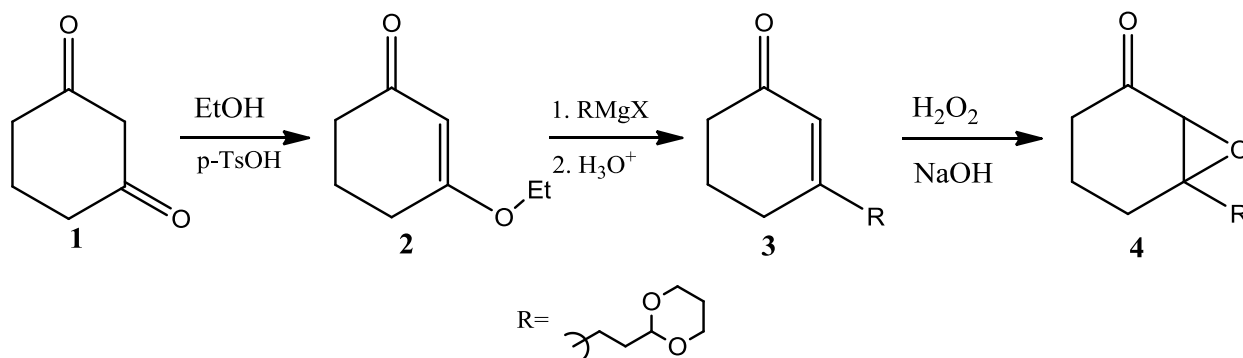


Figure 5: Formation of epoxide precursor from 1,3-cyclohexanedione via a three step synthesis

Compound **1** was treated with p-toluene sulfonic acid and ether to produce **2**, which after distillation left a clear light oil in good yield (66%) and excellent purity. The ¹H NMR for the product (MPF-I-01d) shows the appearance of a 1H singlet at δ=5.30 ppm. This signal is indicative of the vinyl proton formed in the product.

This product was then subjected to a Grignard reaction with an acetal magnesium bromide under anhydrous conditions to produce **3** which after column chromatography produced a light yellow oil. The ¹H NMR for compound **3** (ECD-I-17c-30) shows the appearance of a 1H singlet δ=5.91 ppm and the disappearance of the 1H singlet at δ=5.30 ppm. This is indicative of the conversion of the 3-ethoxycyclohexenone to the new acetal Grignard product (**3**).

Electrophilic epoxidation of **3** using peroxide and base created product **4**. After silica gel column chromatography, the product resulted in a clear oil in 54% yield. The ¹H NMR data for the

²⁰ Dittami, J. P., Ware, R., Nie, X. Y., Nie, H., Ramanathan, H., Breining, S., Reiche, P. (1991). Intramolecular addition reactions of carbonyl ylides formed during photocyclization of aryl vinyl ethers. *The Journal of Organic Chemistry*, 56(19), 5572-5578.

compound shows the disappearance of the 1H vinyl proton peak at 5.91 ppm suggesting the disappearance of **3**. The appearance of a new 1H signal at 3.13 ppm is consistent with the epoxide proton on 2-carbon of the molecule, indicating that the epoxide has been successfully produced.

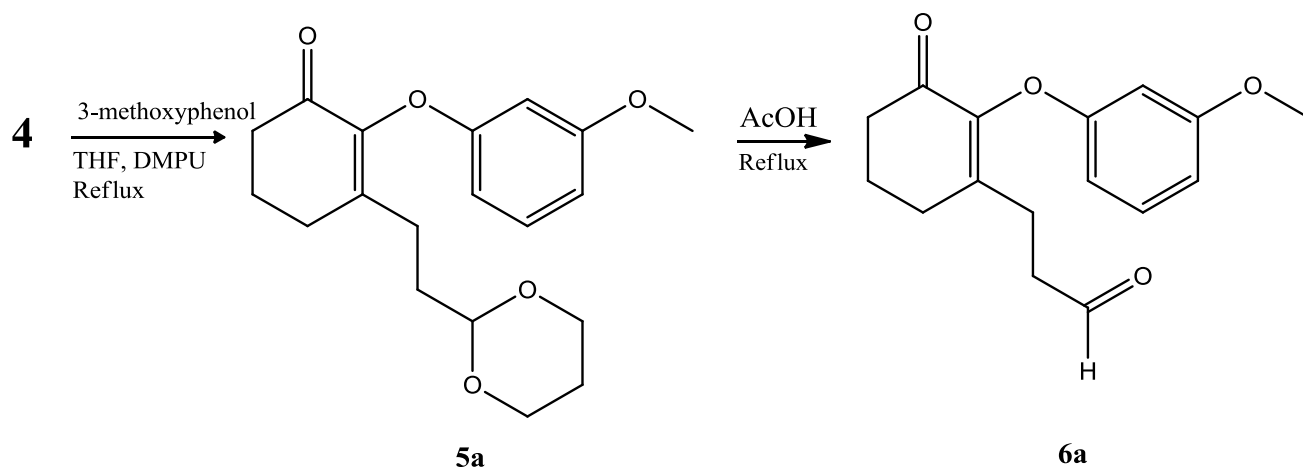


Figure 6: Formation of aryl-vinyl ether precursor for photocyclization

Product **4** could then be coupled using DMPU with a variety of aryl ethers such as naphthol, phenol and other aromatic compounds to produce different aryl-vinyl ethers. One target aryl-vinyl ether product contains a 3-methoxyphenyl ring so coupling of **4** with 3-methoxyphenol was carried out to provide (**5a**) in 23% yield. The ¹H NMR spectrum (AM-III-23c) indicates the success of this reaction in the appearance of key aromatic peaks. The methoxy protons, **a** (see Figure 7) are viewed as a singlet integrating to 3H at $\delta=3.8$ ppm. Signals **c** and **e** appear as 1H signals as doublet of doublet of doublets at $\delta=6.43$ ppm and $\delta=6.45$ ppm respectively. These peaks appear in this multiplicity due to vicinal splitting by **d** ($J=8.2$ Hz) long-range splitting with **b** ($J=2.4$ Hz) and long-range splitting with each other ($J=0.7$ Hz). Signal **b** is viewed as a 1H triplet at $\delta=6.49$. The triplet multiplicity is caused by long-range splitting with **c** and **e** ($J=2.4$ Hz). Finally, the signal accounting for **d** appears as a triplet at $\delta=7.16$ ppm ($J=8.2$ Hz) and integrates to 1H.

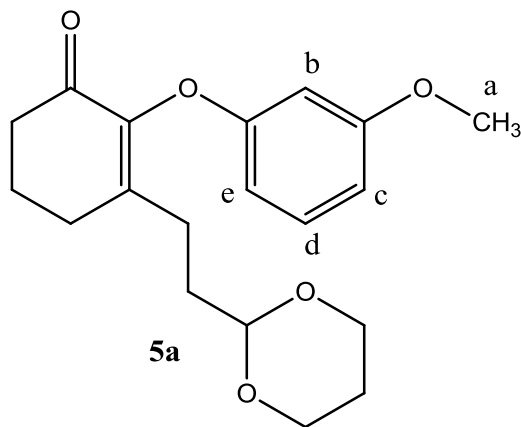


Figure 7: Structure of aryl-vinyl ether with key proton signals (Labeled a-e)

Compound **5a** was then subjected to reflux conditions with acetic acid. These conditions caused the acetal group on the side chain to be deprotected to form compound **6a**, the final precursor necessary for an intermolecular photocyclization. Product **6a** was proven to have formed by the appearance of an aldehyde signal in the ^1H NMR spectra. This signal, seen as a 1H singlet at $\delta=9.76$ ppm indicates that the acetal group has been successfully deprotected leaving the aldehyde functional group in its place.

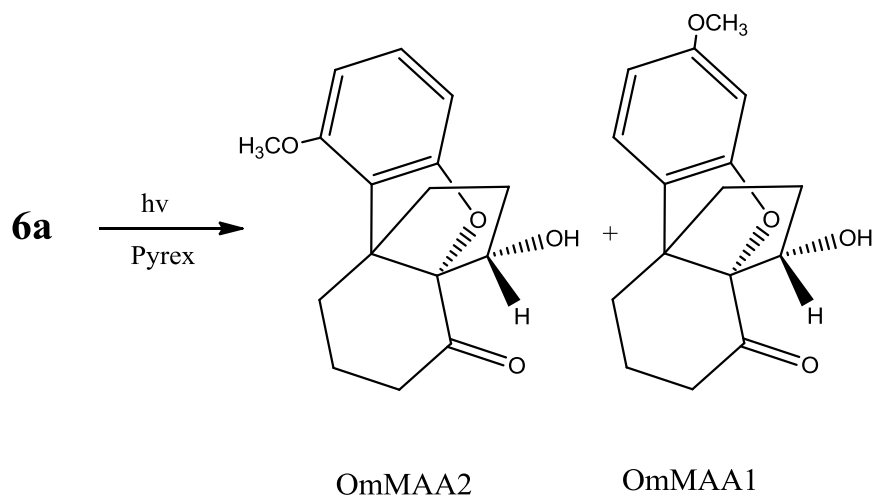


Figure 8: Formation of the photocyclic scaffold via an intramolecular addition of **6a**

Compound **6a** was dissolved in dry toluene and argon gas was bubbled through the solution for 30 minutes after which the reaction mixture was irradiated through Pyrex for 2 hours at room temperature. Degassed conditions were necessary because molecular oxygen can interfere with the intermediate structure in the photocyclization reaction. After purification via silica gel column chromatography, only one stereoisomers was observed through NMR spectroscopy. OmMAA2 was

the observed product, verified via ^1H NMR spectroscopy. The spectrum shows the loss of the 1H aldehyde peak present in **6a** at 9.8 ppm. This observation indicates that intramolecular addition of the side chain has occurred. Another indicative observation is the loss of a phenyl signal from the transition of **6a** to the product. Photocyclization causes an aromatic proton to be shifted from the aromatic to vinyl side of the ether. The spectrum for **6a** shows 4 non-equivalent phenyl signals, while the spectrum of OmMAA2 shows only 3.

OmMAA1 was shown to not have been produced in this particular reaction because of the multiplicity of the phenyl hydrogen signals. If OdMAA1 had been synthesized, the phenyl signals would appear as a singlet 1H peak and two doublet 1H peaks. The NMR data for the photo-products was not consistent with this structure and therefore, cannot be proven to have been synthesized. Further experimental data is needed to fully prove this hypothesis.

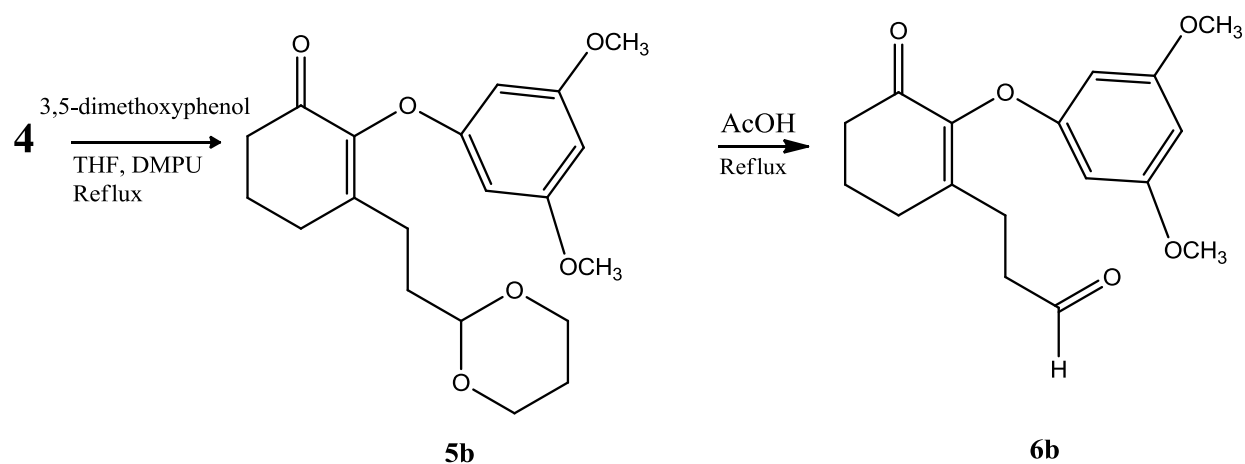


Figure 9: Formation of deprotected aryl-vinyl ether precursor for photocyclization

Product **4** was also coupled to 3,5-dimethoxyphenol for synthesis of a photo-precursor. The coupling of **4** to 3,5-dimethoxyphenol was carried out to provide **5b** in 45% yield. The ^1H NMR spectrum (ECD-I-35c (3)) indicates the success of this reaction in the appearance of key aromatic peaks. The methoxy protons are viewed as a singlet integrating to 6H at $\delta=3.78$ ppm. There is a 1H triplet peak at 6.12 ppm and 2H doublet peak at 6.06 ppm corresponding to the two aromatic proton groups.

Compound **5b** was deprotected following the same procedure as the deprotection of the acetal group on **5a**. This reaction yielded **6b**, the final precursor necessary for an intermolecular photocyclization. Product **6b** was proven to have formed by the appearance of an aldehyde signal in

the ^1H NMR spectra. This signal, seen as a 1H triplet at $\delta=9.77$ ppm indicates that the acetal group has been successfully deprotected leaving the aldehyde functional group in its place.

A second deprotection was attempted on small sample of **5b** using dry acetone and solid iodine at room temperature rather than an acetic acid solution maintained at reflux. These conditions are much milder than the acetic acid deprotection and it was believed that these conditions may provide a better yield. Unfortunately this method of deprotection of acetals showed no change in starting material and no indication of an aldehyde functional group.

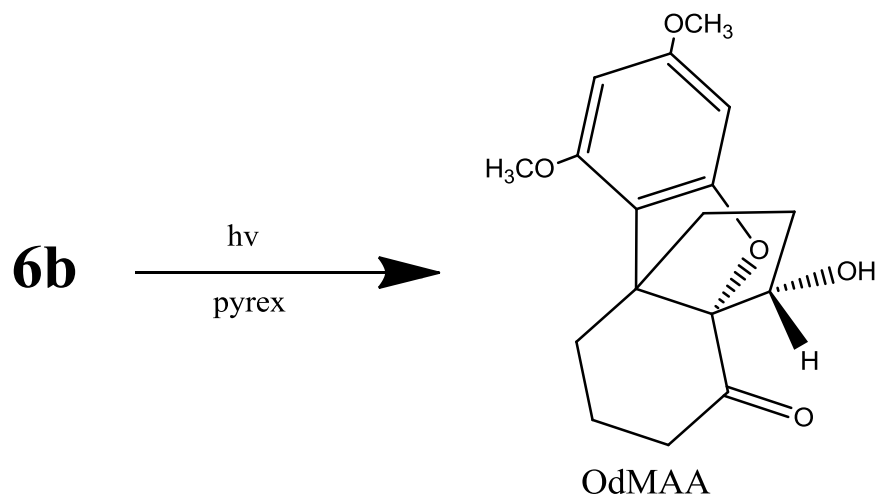


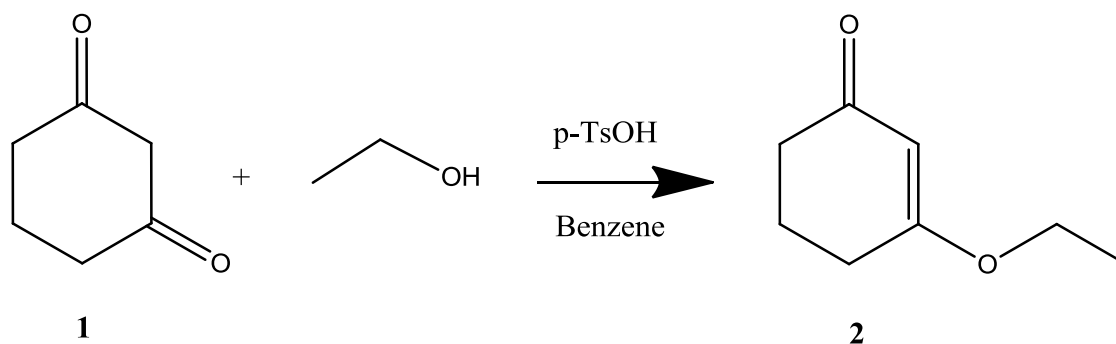
Figure 10: Formation of the photocyclic scaffold via an intramolecular addition of **6b**

Compound **6b** was dissolved in dry toluene and argon gas was bubbled through the solution for 30 minutes after which the reaction mixture was irradiated through Pyrex for 1 hour at room temperature. The product OdMAA was collected as a crude oil and verified via ^1H NMR spectroscopy. The spectrum for this product indicates the transition of **6b** to OdMAA in a few key ways. The first indication is that the methoxy peaks on **6b** were equivalent due to free rotation of the aromatic group, integrating to 6H. After irradiation with Pyrex-filtered light, the methoxy groups were displayed as 2 non-equivalent 3H peaks. This change is due to the rigid structure of OdMAA which does not allow for free rotation of the aromatic group. Further evidence was provided by the lack of an aldehyde signal in the product spectrum, which indicates that intramolecular addition of the side chain occurred.

4. Experimental

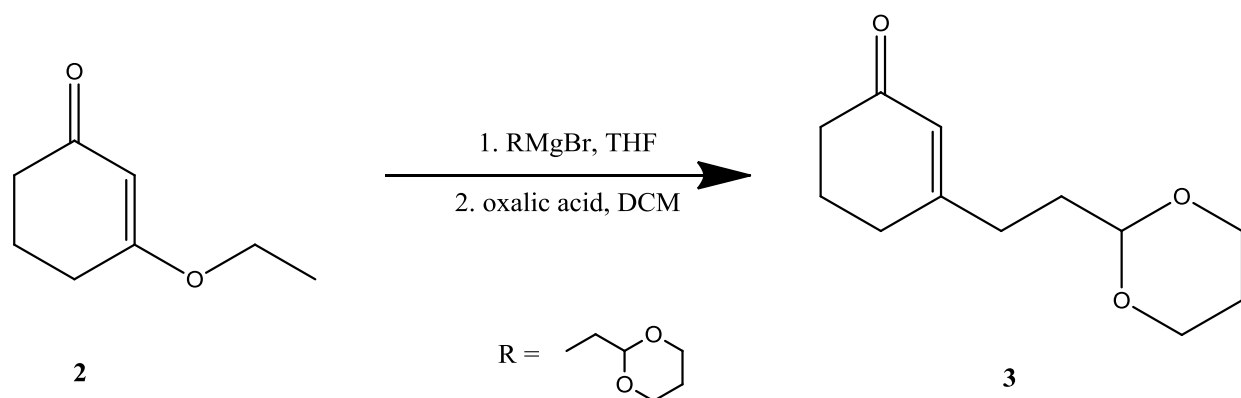
General Methods. High resolution ^1H NMR spectra were obtained using a Bruker 500MHz NMR spectrometer. Chemical shifts are reported in ppm relative to tetramethylsilane at 0.00 ppm. The general experimental procedures included equipment, analytical methods, and solvent and chemical purification processes have been reported elsewhere. Unless otherwise noted, solvent removal was carried out on a rotary evaporator at reduced pressure. Analytical thin-layer chromatography was done on pre-coated silica gel plates (0.25mm thickness) with a 254nm fluorescent indicator and was visualized under a UV lamp and/or by staining with *p*-anisaldehyde. Flash chromatography was run in a silica gel column on an AnaLogix IntelliFlash 280.

3-ethoxy-2-cyclohexen-1-one



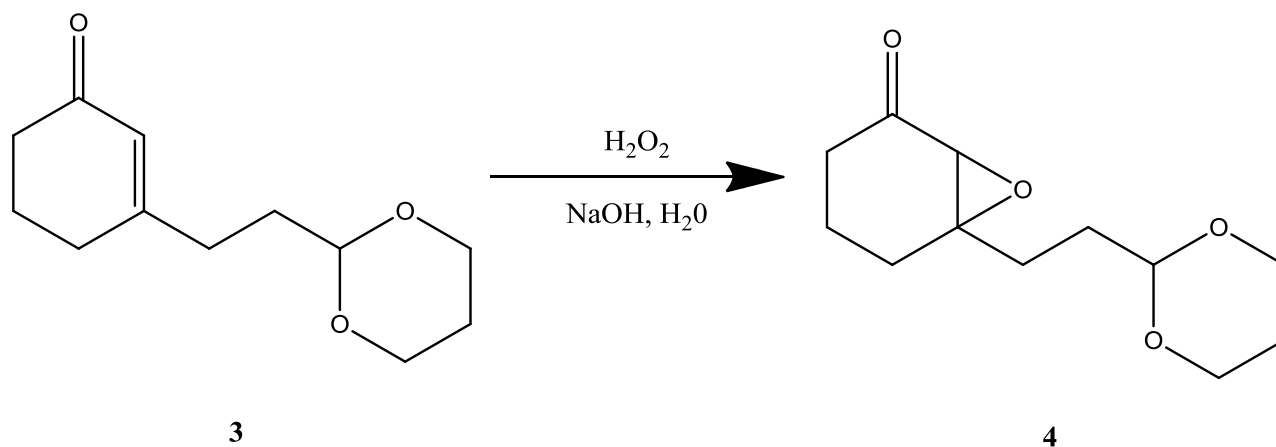
To a 500 mL round bottom flask outfitted with a Dean Stark trap and reflux condenser was added 1,3-cyclohexanedione (30.1 g, 273 mmol) and benzene (250 mL). Ethanol (64 mL, 1093 mmol) was added followed by the addition of paratoluene sulfonic acid (4.75 g, 27.3 mmol). The reaction was maintained at reflux temperature for 24 hours with constant stirring. The mixture was washed with two 25 mL portions of 1% 1M NaOH in brine, water and brine and dried (Na₂SO₄). The solvent was removed under vacuum and the residue was distilled to yield **2** (25.02 g, 66%) as a colorless oil. ¹H NMR (CDCl₃, 600 MHz) δ 1.31 (t, 3H, J = 7.1 Hz), 1.93 (m, 2H), 2.29 (t, 2H, J = 6.7 Hz), 2.36 (t, 2H, J = 6.2 Hz), 3.86 (q, 2H, J = 7.1 Hz), 5.30 (s, 1H) (MPF-I-1d).

3-[2-(1,3-Dioxan-2-yl)ethyl]-2-cyclohexen-1-one



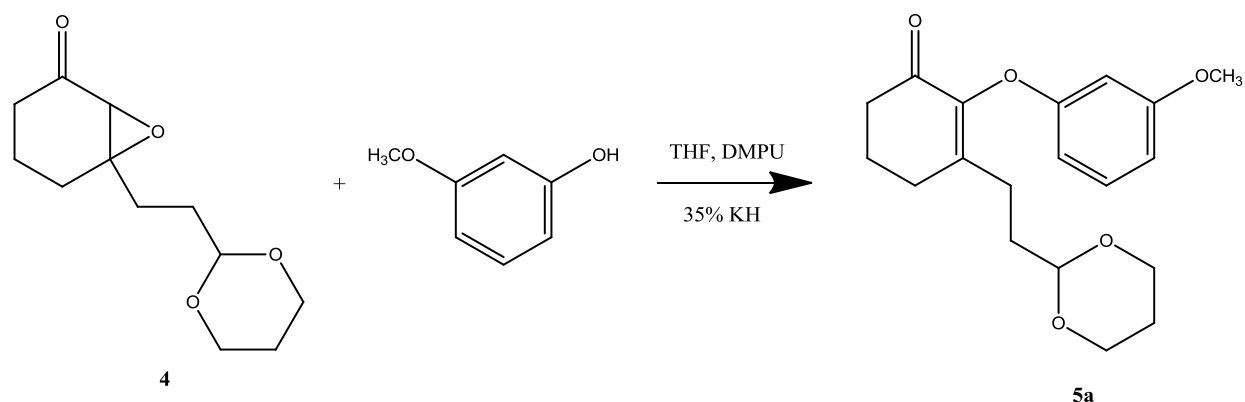
To a dry 100 mL three-neck flask equipped with a reflux condenser, was added magnesium turnings (0.110 g, 45.3 mmol) and THF (20 mL) followed by the slow addition of 2-(2-bromoethyl)-1,3-dioxane (5.15 mL, 38.0 mmol). The reaction was maintained at reflux temperature for 10 minutes and then cooled to 0° C. A solution of 3-ethoxy-2-cyclohexen-1-one (5.0 mL, 34.3 mmol) in dry THF (13 mL) was slowly added dropwise. The mixture was stirred at room temperature for 24 hours. THF was removed under vacuum and the residue was partitioned between dichloromethane and saturated aqueous oxalic acid. The aqueous phase was washed with dichloromethane and the combined organic phases were washed with distilled water and brine and then dried over Na₂SO₄. Solvent was removed under vacuum to yield a dark crude oil. The crude product was purified by chromatography on silica gel (hexane/ethyl acetate (1:1)) to provide **3** (4.99 g, 69%). ¹H NMR (CDCl₃, 600 MHz) δ 1.82 (m, 2H), 2.01 (p, 2H, J = 6.4 Hz), 2.10 (m, 2H), 2.36 (m, 6H) 3.78 (m, 2H), 4.13 (m, 2H), 4.57 (t, 1H, J = 4.9 Hz), 5.91 (m, 1H) (ECD-I-27c2 (10)).

6-(2-(1,3-dioxan-2-yl)-7-oxabicyclo[4.1.0]heptan-2-one



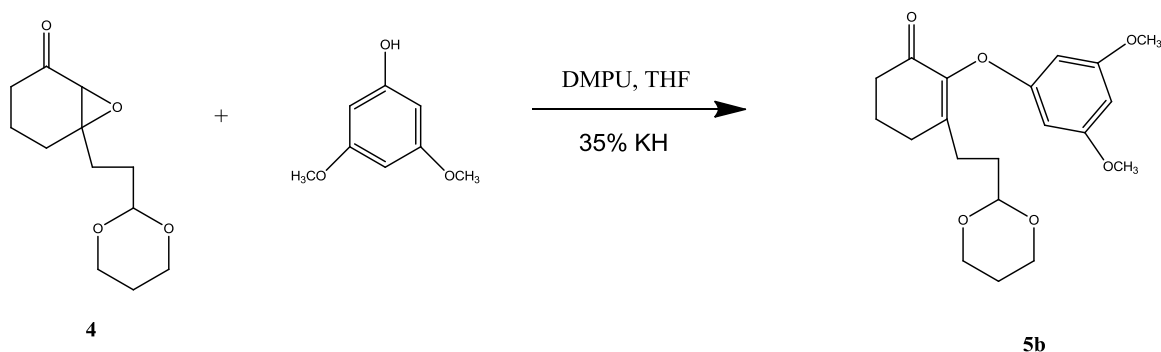
To a 100mL round bottom flask, a mixture of **3** (1.98 g, 9.42 mmol), methanol (9.0 mL) and H_2O_2 (30%, 2.4 mL, 23.54 mmol) was added. The reaction mixture was cooled to 10°C in an ice bath followed by the subsequent dropwise addition of 1M NaOH (9.4 mL, 9.4 mmol) over a period of 15 minutes. The reaction was stirred for 24 hours at room temperature. The product was extracted with dichloromethane and the aqueous phase was further washed with dichloromethane. The organic phases were combined and washed with water and brine and dried (Na_2SO_4). The solvent was removed under vacuum to yield a crude oil. The crude product was purified by chromatography on silica gel deactivated with triethylamine (hexane/ethyl acetate (4:1)) to provide **4** (1.14 g, 54%) ^1H NMR (CDCl_3 , 600 MHz) δ 1.65 – 2.14 (m, 11H), 2.53 (dt, 1H, $J = 17.6$ Hz, 4.3 Hz), 3.13 (s, 1H), 3.77 (m, 2H), 2.10 (m, 2H), 4.56 (t, 1H, $J = 4.6$) (ECD-I-37a).

3-(2-(1,3-dioxan-2-yl)ethyl)-2-(3-methoxyphenoxy)cyclohexenone



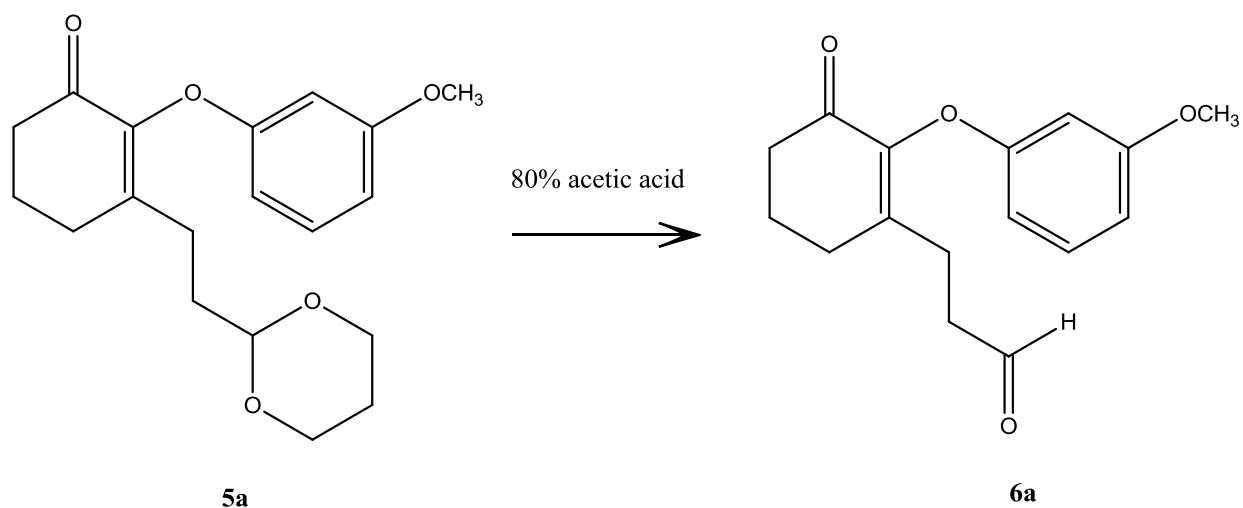
To a flame-dried 10 mL three-neck flask outfitted with a reflux condenser, **4** (0.5 g, 2.21 mmol) was added to THF (1 mL). In a separate dried 5 mL pear-shaped flask, 3-methoxyphenol (0.264 g, 2.48 mmol), THF (1 mL) and DMPU (1 mL, 8.29 mmol) was added. To this solution, KH in mineral oil (35%, 0.0044 g, 1.1 mmol) was added. This solution was added to the epoxide solution and maintained at reflux for 48 hours. The solvent was removed under vacuum and partitioned between DCM and 10% NaOH in brine. The organic layer was washed with distilled water and brine and dried (Na₂SO₄). The solvent was removed and the crude product was dissolved in ether to remove excess DMPU, washed with water and brine and dried over Na₂SO₄. Ether was removed under vacuum. The crude product was purified by chromatography on silica gel (hexane/ethyl acetate (7:3)) to provide **5a** (0.20 g, 25%) as a white solid. ¹H NMR (CDCl₃, 600 MHz) δ 1.79 (m, 2H), 2.01 (m, 4H), 2.40 (m, 2H), 2.56 (m, 4H), 3.72 (m, 2H), 3.80 (s, 3H), 4.08 (m, 2H), 4.49 (t, 1H, J = 5.1 Hz), 6.43 (ddd, 1H, J = 8.3 Hz, 2.4 Hz, 0.7 Hz), 6.49 (t, 1H, J = 2.4 Hz), 6.55 (ddd, 1H, J = 8.3 Hz, 2.4 Hz, 0.7 Hz), 7.16 (t, 1H, J = 8.2 Hz) (AM-III-23c).

3-(2-(1,3-dioxan-2-yl)ethyl)-2-(3,5-dimethoxyphenoxy)-cyclohex-2-enone



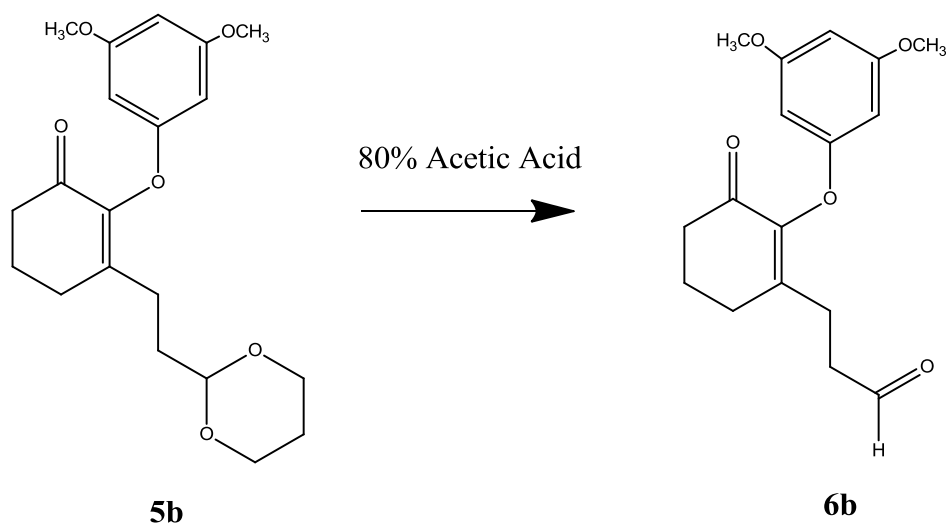
To a flame-dried 50 mL three-neck flask outfitted with a reflux condenser, was added DMPU (1 mL) and a solution of 3,5-dimethoxyphenol (0.499 g, 3.24 mmol) in dry THF (1 mL). To this mixture was added KH in mineral oil (35%, 0.052 g, 1.35 mmol). When reaction was completed, a solution of **4** (0.61 g, 2.70 mmol) and dry THF (2 mL) was added. The mixture was maintained at reflux for 24 hours. The solvent was removed under vacuum and partitioned between DCM and 10% NaOH in brine. The organic layer was washed with distilled water and brine and dried over Na₂SO₄. The solvent was removed and the crude product was dissolved in ether to remove excess DMPU, washed with water and brine and dried (Na₂SO₄). Ether was removed under vacuum. The crude product was purified by chromatography on silica gel (hexane/ethyl acetate (3:1)) to provide **5b** (0.44 g, 45%) as a light yellow oil. (¹H NMR (CDCl₃, 600 MHz) δ 1.35 (m, 1H), 1.79 (m, 2H), 2.07 (m, 3H), 2.39 (m, 2H), 2.55 (m, 4H), 3.74 (m, 2H), 3.78 (s, 6H), 4.08 (m, 2H), 4.50 (t, 1H, J = 5.0 Hz), 6.06 (d, 2H, J = 2.1 Hz), 6.12 (t, 1H, J = 2.2 Hz) (ECD-I-35c (3)).

3-(2-(3-methoxyphenoxy)-3-oxocyclohex-1-en-1-yl)propanal



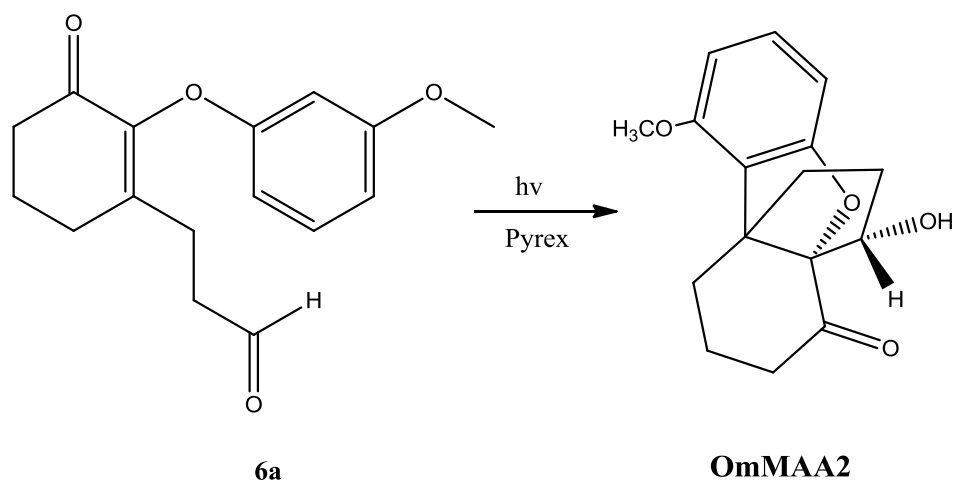
To a 50 mL round bottom flask, **5a** (0.20 g, 0.602 mmol) and acetic acid (80% , 11 mL) was added. The solution was heated gently at approximately 65°C with constant stirring for 48 hours. The product was neutralized with saturated sodium bicarbonate (40 mL), extracted with dichloromethane, washed with water and brine, and dried (Na_2SO_4). Solvent was removed under vacuum. The crude product was purified by chromatography on silica gel (hexane/ethyl acetate (1:1)) to provide **6a** (0.12 g , 73%). ^1H NMR (CDCl_3 , 600 MHz) δ 2.10 (m, 2H), 2.54-2.70 (m, 8H), 3.81 (s, 3H), 6.42 (ddd, 1H, $J = 8.3$ Hz, 2.4 Hz, 0.7 Hz), 6.45 (t, 1H, $J = 2.4$ Hz), 6.57 (ddd, 1H, $J = 8.2$ Hz, 2.4 Hz, 0.7 Hz), 7.17 (t, 1H, $J = 8.2$ Hz), 9.76 (s, 1H) (AM-III-27c).

3-(2-(3,5-dimethoxyphenoxy)-3-oxocyclohex-1-en-1-yl)propanal



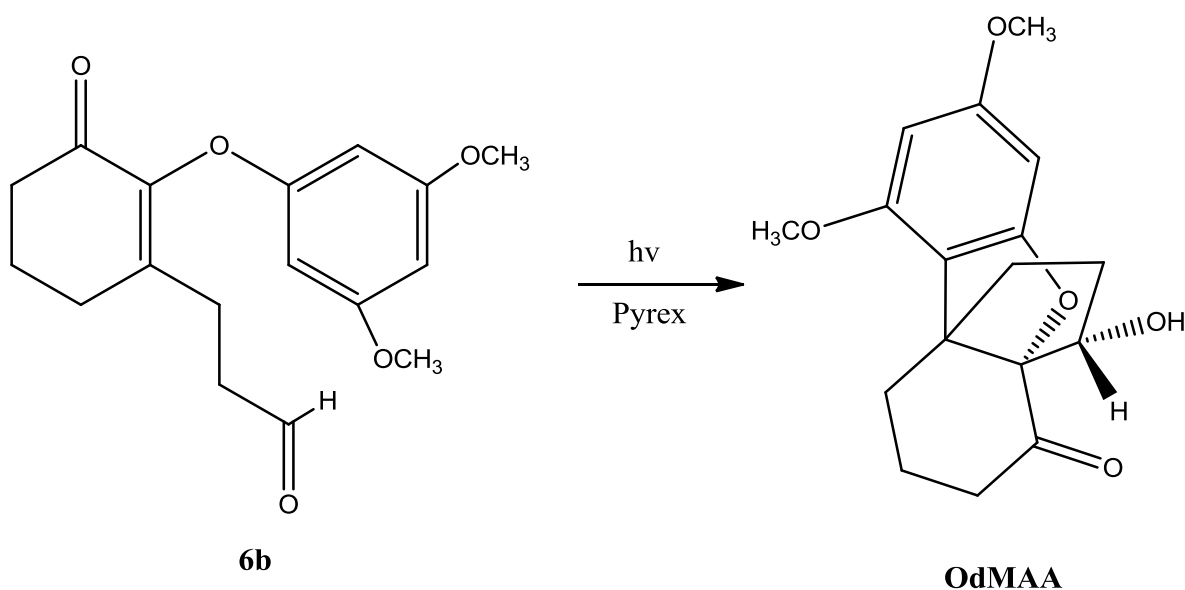
To a 50 mL round bottom flask, **5b** (0.44 g, 1.21 mmol) and acetic acid (80%, 20 mL) was added. The solution was heated gently at a 65°C for 48 hours. The product was neutralized with saturated sodium bicarbonate (40 mL), extracted with dichloromethane, washed with water and brine, and dried (Na_2SO_4). Solvent was removed under vacuum. The crude product was purified by chromatography on silica gel (hexane/ethyl acetate (1:1)) to provide **6b** (0.03 g, 8%) as a light yellow oil. ^1H NMR (CDCl_3 , 600 MHz) δ 2.07-2.15 (m, 2H), 2.53-2.71 (m, 8H), 3.78 (s, 6H), 6.04 (d, 2H, $J = 2.2$), 6.14 (t, 1H, $J = 2.2$), 9.77 (t, 1H, $J = 1.1$) (ECD-I-39c (11)).

OmMAA2



Compound **6a** (0.032 g, 0.117 mmol) was dissolved in dry toluene (25 mL) in an 18 x 150 mm test tube. Argon gas was bubbled through the solution for 30 minutes after which the reaction mixture was irradiated through Pyrex for 2 hours at room temperature. Solvent was removed under vacuum, and the resulting product was purified by column chromatography on silica gel (hexane/ethyl acetate (4:1)) to provide OmMAA2 as a yellow oil (0.005 g, 16%). ¹H NMR (CDCl₃, 600 MHz) δ 1.72-1.80 (2H, m), 1.88 (1H, m), 1.95-2.11 (4H, m), 2.46 (2H, m), 3.74 (3H, s), 4.24 (1H, m), 6.40 (1H, d, *J* = 8.0 Hz), 6.49 (1H, dd, *J* = 8.0 Hz, 0.8 Hz), 7.05 (1H, t, *J* = 8.0 Hz) (AM-III-39d (2)).

OdMAA



Compound **6b** (0.030 g, 0.099 mmol) was dissolved in dry toluene (25 mL) in an 18 x 150 mm test tube. Argon gas was bubbled through the solution for 30 minutes after which the reaction mixture was irradiated through Pyrex for 1 hour at room temperature. Solvent was removed under vacuum to provide OdMAA as a crude yellow oil (0.029 g, 97%). ^1H NMR (CDCl_3 , 600 MHz) δ 1.54 (1H, m), 1.77-1.85 (2H, m), 1.99-2.06 (3H, m), 2.10-2.17 (2H, m), 2.55 (2H, m), 3.79 (3H, s), 3.81 (3H, s), 4.32 (1H, m), 6.08 (1H, d, $J = 2.0$ Hz), 6.18 (1H, d, $J = 2.0$ Hz) (ECD-I-47a).

References

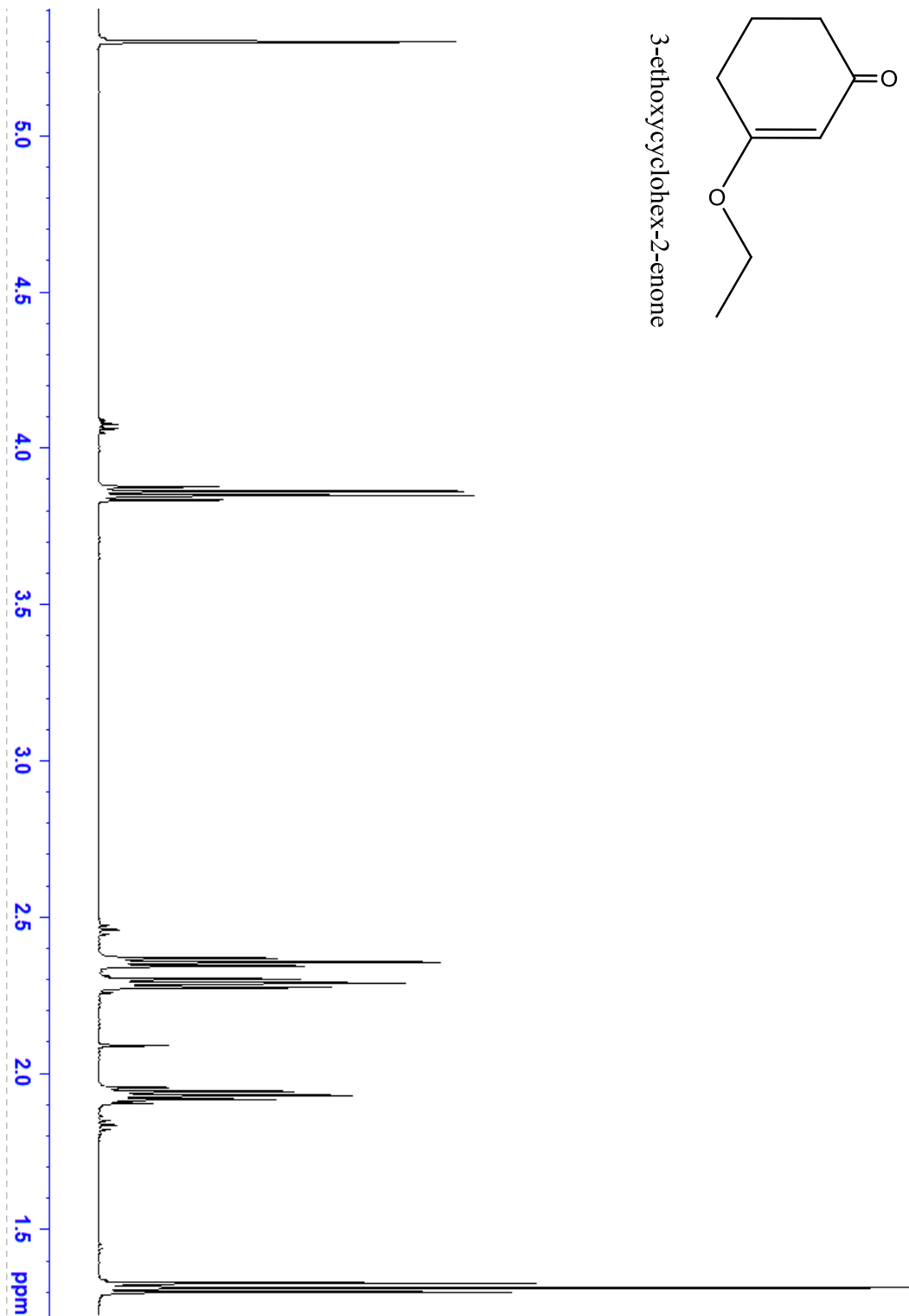
- Cao, D., Liu, S., Xu, Q., Lu, H., Huang, J., Hu, Q., & Liang, Y. (2012). Large-scale prediction of drug-target interactions using protein sequences and drug topological structures. *Analytica Chimica Acta*, 752, 1.
- Casey, A. F., & Parfitt, R. T. (1986). *Opioid analgesics: Chemistry and receptors*. New York: Plenum Publishing Corporation.
- Daylight Theory Manual*. (August 1, 2011). Daylight Chemical Information Systems, Inc.
- Dittami, J. P. (2003). Explorations of the heteroatom directed photoarylation reaction. A review of the photoinitiated intramolecular cycloaddition reactions of ylide systems. *Cheminform*, 34(45)
- Dittami, J. P., Ware, R., Nie, X. Y., Nie, H., Ramanathan, H., Breining, S., Reiche, P. (1991). Intramolecular addition reactions of carbonyl ylides formed during photocyclization of aryl vinyl ethers. *The Journal of Organic Chemistry*, 56(19), 5572-5578.
- Fruchart, J. (2007). Novel peroxisome proliferator activated receptor-alpha agonists. *The American Journal of Cardiology*, 100(11 A), n41.
- Grabowski, K., Baringhaus, K., & Schneider, G. (2008). Scaffold diversity of natural products: Inspiration for combinatorial library design. *Natural Product Reports*, 25(5), 892.
- Guner, O. F. (Ed.). (2000). *Pharmacophore perception, development, and use in drug design* International University Line.
- Harvey, A. L. (2008). Natural products in drug discovery. *Drug Discovery Today*, 13(19), 894-901.
- Keiser, M. J., Tran, T. B., Whaley, R., Glennon, R. A., Hert, J., Thomas, K. L. H., Matos, R. C. (2009). Predicting new molecular targets for known drugs. *Nature*, 462(7270), 175-181.
- Koehn, F. E., & Carter, G. T. (2005). The evolving role of natural products in drug discovery. *Nature Reviews Drug Discovery*, 4(3), 206-220.
- Mandard, S., Müller, M., & Kersten, S. (2004). Peroxisome proliferator-activated receptor alpha target genes. *Cellular and Molecular Life Sciences: CMLS*, 61(4), 393.
- Patani, G. A., & LaVoie, E. J. (1996). Bioisosterism: A rational approach in drug design. *Chemical Reviews*, 96(8), 3147-3176.
- Planavila, A., Iglesias, R., Giralt, M., & Villarroya, F. (2011). Sirt1 acts in association with PPAR α to protect the heart from hypertrophy, metabolic dysregulation, and inflammation. *Cardiovascular research*, 90(2), 276-284

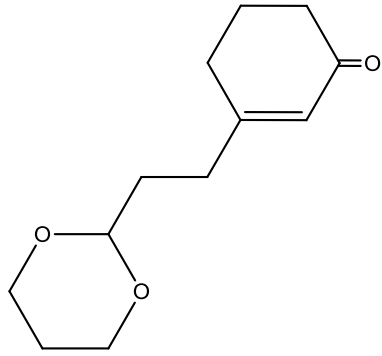
Rogers, D., & Hahn, M. (2010). Extended-connectivity fingerprints. *Journal of Chemical Information and Modeling*, 50(5), 742.

Schultz, A. G. (1983). Photochemical six-electron heterocyclization reactions. *Accounts of Chemical Research*, 16(6), 210-218.

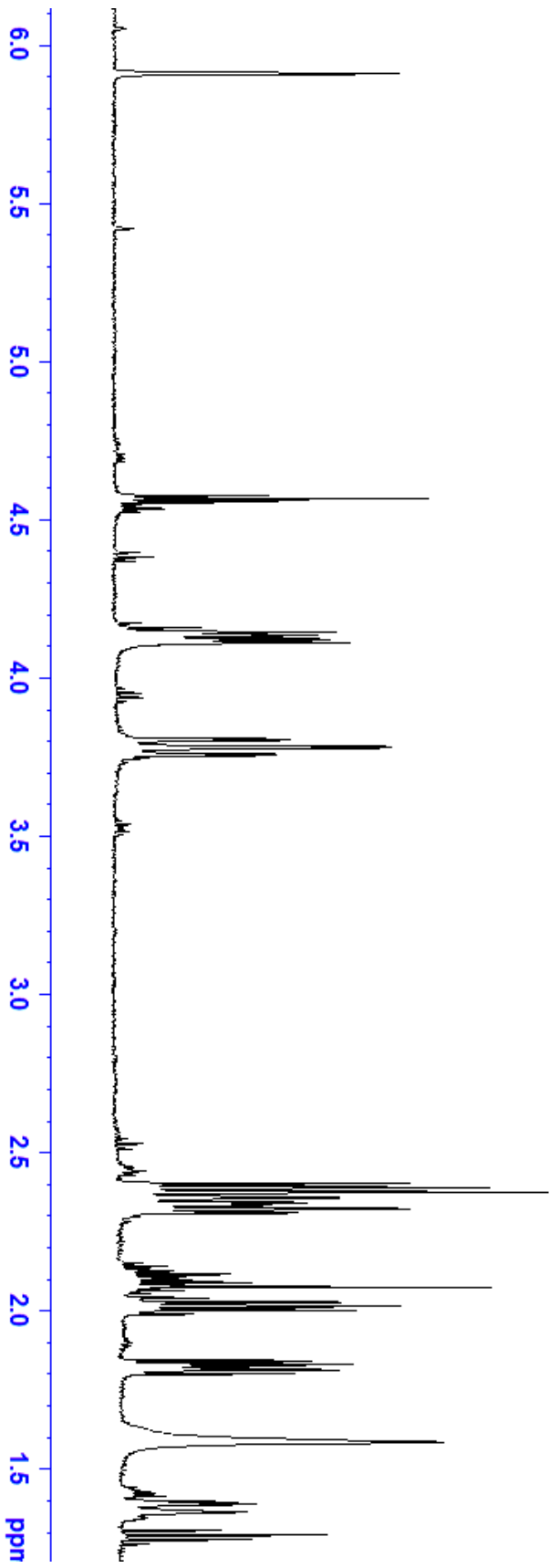
Appendices

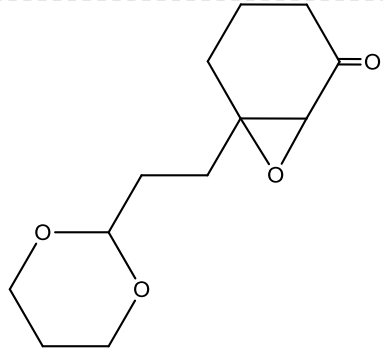
Appendix A: NMR Data



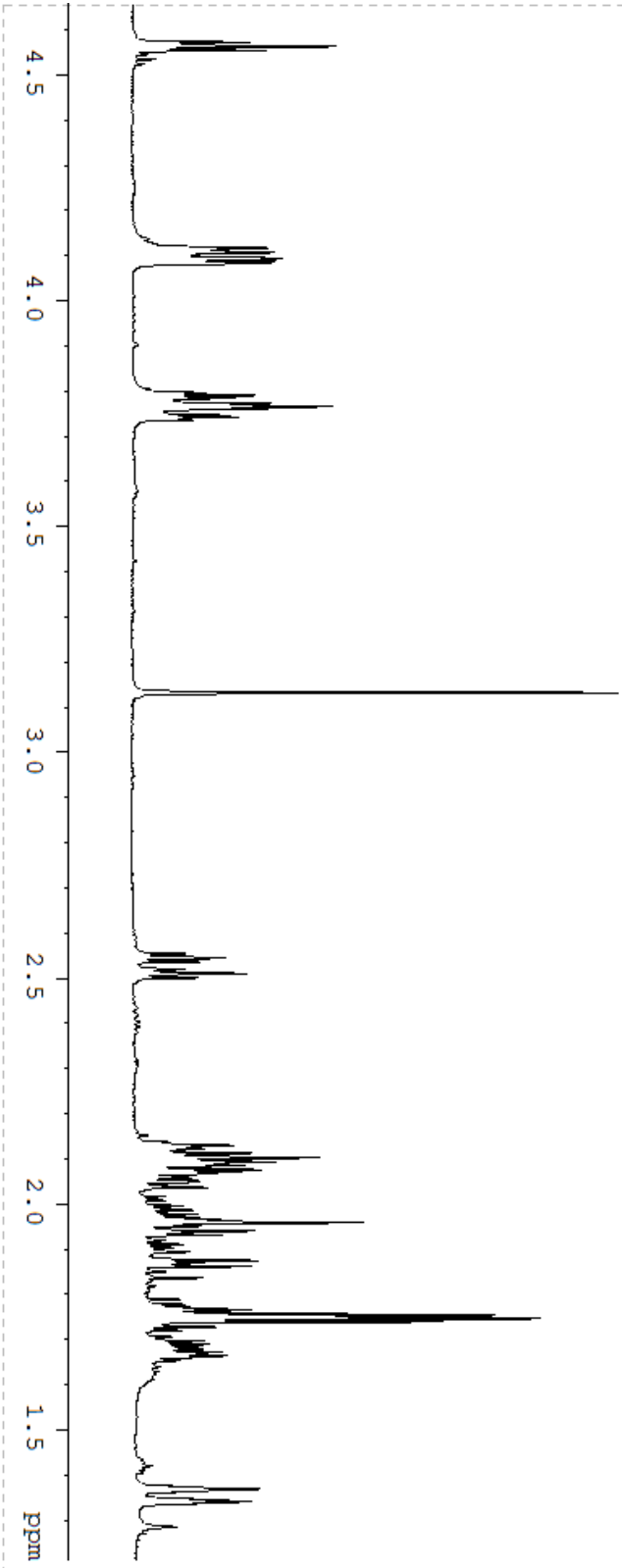


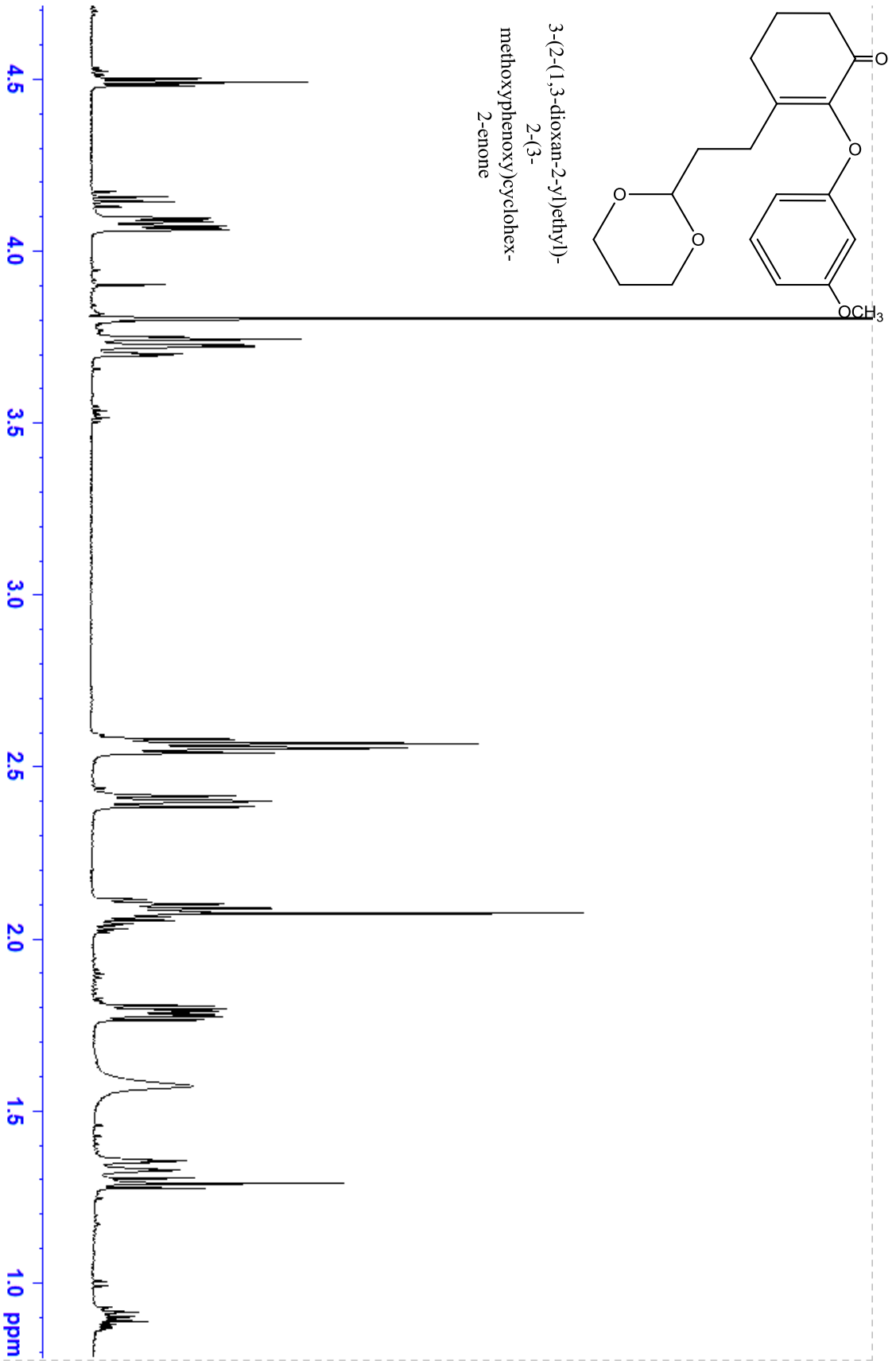
3-(2-(1,3-dioxan-2-yl)ethyl)cyclohex-2-enone

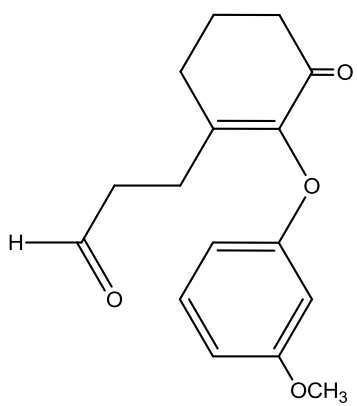




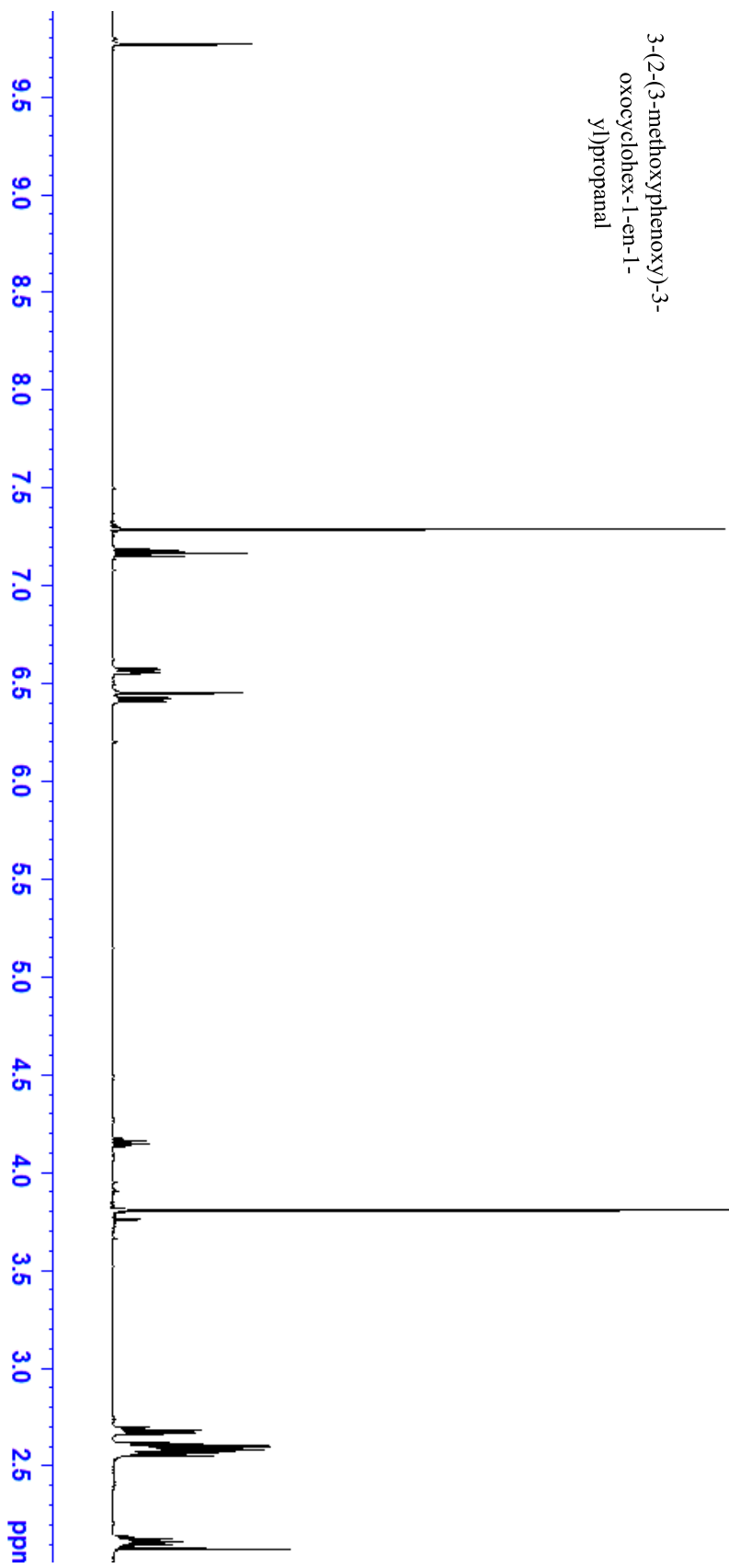
6-(2-(1,3-dioxan-2-yl)ethyl)-
7-oxabicyclo[4.1.0]heptan-
2-one

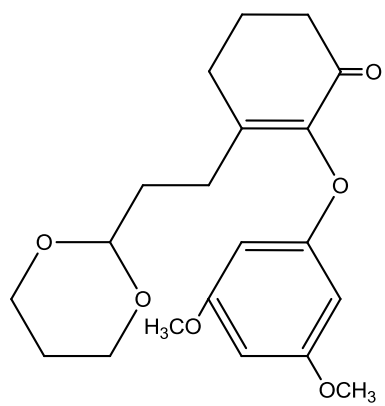






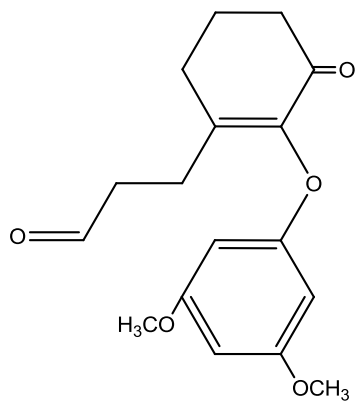
3-(2-(3-methoxyphenoxy)-3-oxocyclohex-1-en-1-yl)propanal





3-(2-(1,3-dioxan-2-yl)ethyl)-
2-(3,5-
dimethoxyphenoxy)cyclohex-
2-en-1-one





3-(2-(3,5-dimethoxyphenoxy)-3-oxocyclohex-1-en-1-yl)propanal

